

Scattering of ultrasonic longitudinal waves in unidirectional composites

Daniel Marcus Giglioli de Oliveira¹, Vanessa Vieira Gonçalves¹, and Auteliano Antunes dos Santos¹

¹ University of Campinas, Rua Mendeleev, 200, Cidade Universitária, Zeferino Vaz, 13083-860 Campinas, Brazil.

Abstract: The stress distribution and the elastic constants can be determined using the velocity of ultrasonic waves travelling inside the material. The relationship between these parameters is found from the acoustoelasticity theory. However, the waves propagating in heterogeneous and anisotropic materials, as in composite materials, undergo considerable dispersion. Knowing this effect is particularly important for stress measurement, since the dispersion could lead to an erroneous safety estimative. The purpose of this study is to evaluate the dispersion of longitudinal ultrasonic waves in unidirectional carbon-fiber composites, aiming to model its effect on the wave propagation velocity. A special developed sample with 24 faces was built and measurements were taken in angles from 0° up to 90° from the fiber direction using through transmission technique. The results show that there are significative differences in the propagation velocity depending on the angle and call for a very strict control of the transducers positions during stress measurements.

Keywords: Composite materials, non-destructive tests, ultrasound, stress measurement, wave scattering.

INTRODUCTION

Composite materials are used in various segments such as aerospace, automotive, naval, sports and others. Because of this, there is a great commitment with studies directed to these materials. Among these studies one can highlight those directed to non-destructive tests (NDT) such as x-ray and ultrasound. This latter has proven to be advantageous because, unlike the other methods, it is a low-cost technique for which highly skilled operators are not required. Amongst the ultrasound applications the one that uses the acoustoelasticity principle should be mentioned, because it allows to relate the velocity of the wave with the stress to which the material is submitted (Santos and Bray, 2002). The modern bases of acoustoelasticity were established by Hughes and Kelly (1953), Toupin and Bernstein (1961), Thurston and Brugger (1964), and Pao and Gamer (1985). The ultrasonic method is also employed in the detection of defects and to obtain elastic constants.

The current research about the method aims to understand the behavior of ultrasonic waves in composite materials. Parameters such as amplitude, scattering and attenuation have been evaluated for particular types of composites. The attenuation of longitudinal waves has relation with scattering and absorption caused by viscoelastic properties of the constituent phases of composite materials. By numerical analysis Biwa et al (2002) showed the scattering of transversal waves in the composites and its relationship with frequency and size of constituents. The attenuation phenomenon was also studied using the ultrasonic immersion method through the comparison of the attenuation between composite of polymeric matrix and a similar one, but reinforced with long fibers (Baudouin and Hoster, 1996).

In relation to the amplitude of wave signal, this parameter is widely used in detection of a defect. It is possible to identify its position by signal reflections. Yu et al (2017) studied guided waves in quasi-isotropic composites to determine defects in a curved form. They verified that the change in amplitude is small in the presence of delamination when analyzing this discontinuity by energy variation. They also obtained adequate results for crack detection analyzing the attenuation.

The analysis of scattering of ultrasonic longitudinal waves in unidirectional composites makes it possible to find the path traveled by the wave according to the change in the angle of the fiber, as well as understand the sensitivity and energy of the signal captured by transducer. This may justify the search for the best position of the transducer for detection of defects and stress measurement when used for unidirectional and multidirectional composites.

In this context, the objective of this study is to relate the behavior of the longitudinal ultrasonic wave with the orientation of the fiber of a unidirectional carbon/epoxy composite material by the measuring of the reception of the wave at different angles from the emission line. As a result, it is expected to apply the findings in simulations, ultrasonic propagation modeling, and, consequently, in the stress prediction in composite materials using the acoustoelasticity theory.

Materials and Methods

One sample of polygonal form with 24 faces was used for this study. It is a unidirectional composite specimen manufactured with prepreg of carbon fiber/epoxy resin (HexTow® AS4 and HexPly® 8552). This sample has 196.73 mm between parallel faces and was made with 96 layers of prepreg. Its thickness is 17.70 mm. The manufacturing process of this sample is more detailed in Santos et al (2014) and Rodovalho (2012). The faces of the sample were cut every 15° with respect to the fiber. The properties of material are shown in Tab.1 and its form in Fig.1 and Fig.2(c).

Table - 1: Properties of prepreg Hexply® AS4/8552 23

Lamina density (kg/m ³)	1590
Nominal fiber volume (%)	58.5
Lamina thickness (mm)	0.187
Longitudinal elastic modulus (GPa)	142
Transversal elastic modulus (GPa)	9.5
Shear modulus (GPa)	5.0
Longitudinal tensile strength (MPa)	2336
Transversal tensile strength (MPa)	81
Shear strength (MPa)	114

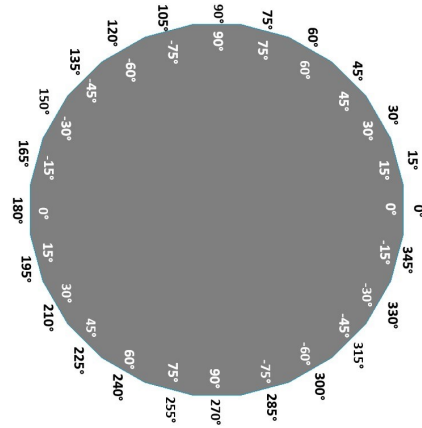


Figure 1 - Polygonal sample and its angles

The Fig.2(a) is indicating the direction of fibers in unidirectional polygonal sample, and Fig.2(b) shows the angle θ with respect to fiber, which ranges from 0° to 360°, in steps of 15°.

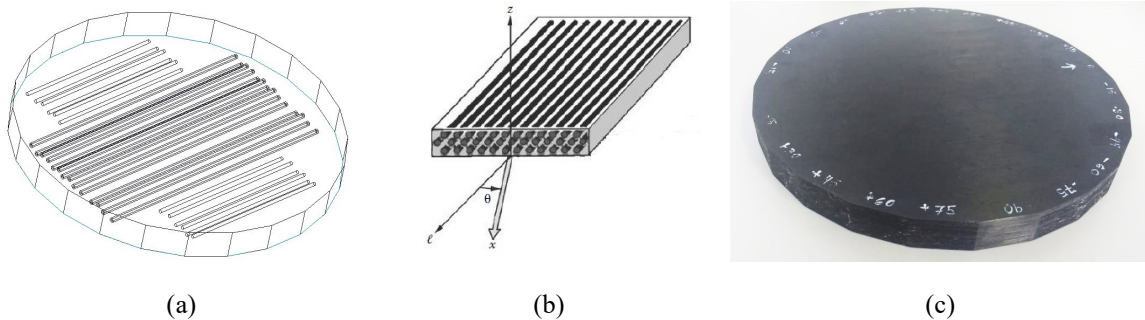


Figure 2 – Polygonal sample details. (a) fibers in the sample (b) angle to the fiber (c) picture of the sample

The measurements of longitudinal waves were performed using two transducers manufactured by Panametrics/Olympus®, model A103S, frequency of 1.0 MHz. The emitting and receiving of signal were controlled by a portable device pulser/receiver Ultratek®, model UT350, sampling rate of 50 MHz. This device was connected to the USB port in a laptop. The data acquisition and waveform analysis occurred using a program developed by the research group using Labview®. The TOF (time-of-flight) was obtained measuring the time at the second intersection with the zero amplitude, after the first peak of the wave train. This point was chosen because the first pulse corresponds to the longitudinal wave and the second zero crossing is easy to identify in this pulse.

As mentioned by Santos et al (2014), the velocity of wave can be affected by changes in temperature. Because of that, the temperature was controlled at the test site, maintained in 23°C (+/- 1°C). The temperature was controlled using an air conditioning system. Before measuring, the temperatures of the sample and of the measurement system are required to be stable. The monitoring of temperature in the sample was made with a thermocouple type K, through data acquisition board NI-9211. The scheme of the measurement system is shown in Fig.3 and Fig.4.

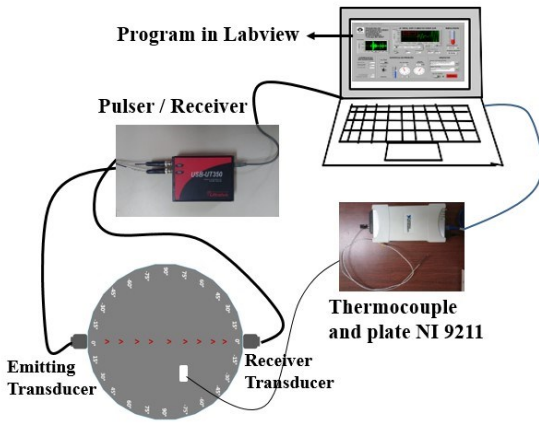


Figure 3 – Measurement System

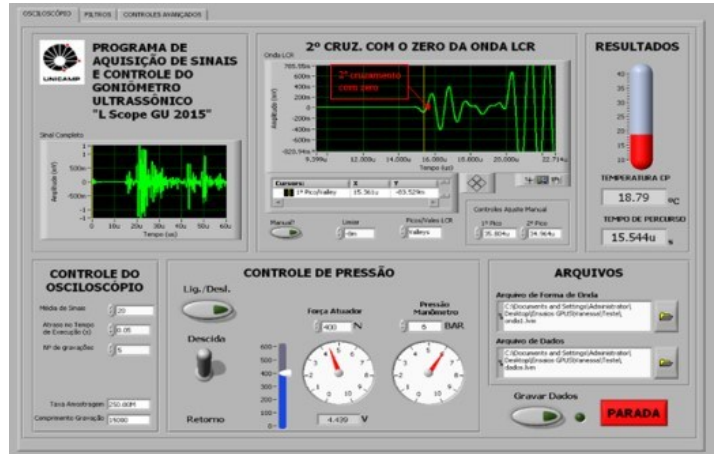


Figure 4 – Program screen

Prior to measurement on the samples, the transducers were calibrated using standard Panametrics / Olympus® block type TB 1054-1 conforming to ASTM E 164 IIW. The calibration was performed by means of three measurements of velocity through an echo pulse in the standard block. The block is shown in Figure 5.

To calibrate the transducers, a standard block type 1 of Panametrics / Olympus® Model TB 1054-1 was used, according to ASTM E 164 IIW. The calibration was performed by means of three measurements of velocity through an pulse-echo arrangement in the standard block, shown in Figure 5.



Figure 5 – Standard block.

The first test was performed with the emitter transducer positioned in direction 0°-180°, face 0° (Fig.1), the receiver transducer was positioned on the opposite face and in each measurement, it is moved to adjacent sides in counterclockwise. Then, it is positioned again in opposite face (180°) and moved clockwise. The same procedure was made with emitter transducer in face -45° (referent to 135° in Fig.1), +45° (referent to 225°) and 90° (referent to 270°). Two measurements were performed in each face of sample. In each measurement the program saves five values of TOF for the longitudinal wave and a file with corresponding amplitudes. This can be used to reconstruct the signal measured for analysis purpose. The values of TOF analyzed in this work result in an average from the 10 values recorded.

RESULTS AND DISCUSSIONS

The first parameter analyzed was the travel time of the longitudinal wave. As mentioned in materials and methods, the transducer that emits the signal was fixed in a position, while the receiver transducer was moved for others faces. As mentioned before, the emitter transducer was placed in direction 0°, -45°, +45° and 90° from the fiber. The results are as follow.

Emitter at 0°

With the emitter at position 0° (equivalent to 180° in Fig.1) and the receiver on the opposite and parallel side, the shortest time of propagation for the longitudinal wave was obtained. The graph of Fig. 6(a) shows the times of flight for each direction where the receiving transducer was positioned, and Fig.6(b) the initial position of transducers.

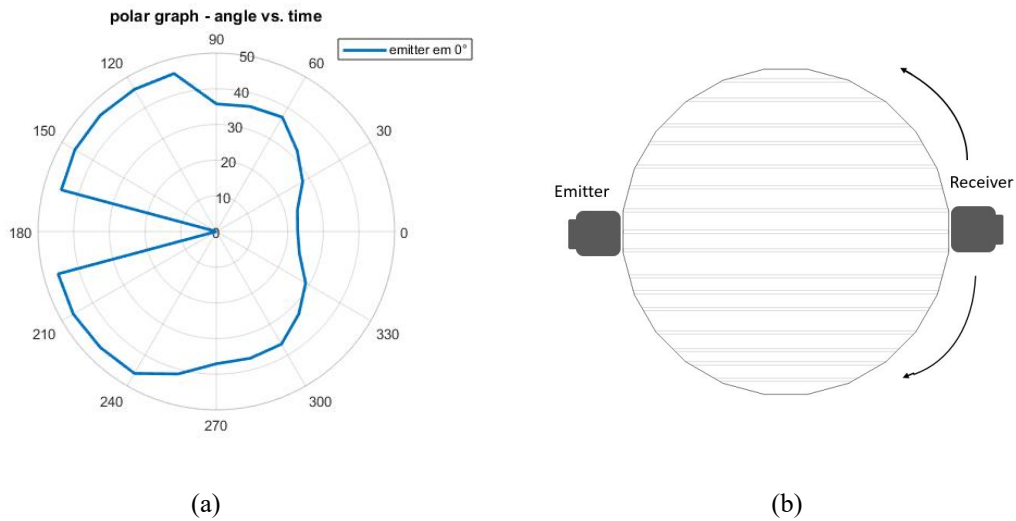


Figure 6 – Results for emitter in 0°. (a) Time vs. position graph (b) Position of the transducer in relation to fiber

In the graph of Fig.6(a), the shortest time was found in the direction directly opposite to the emitter, that is, in the direction of the fiber (0°), measured 22,8 μs. A little variation of 5 μs to more appears when receiver transducer is in 30° and 6 μs when is in -30° (330°). For other directions, the value measured is much higher. The largest difference occurs between the angles -75° (105°) to 15° (165°) and between angles 15° (195°) to 60° (240°), where the difference reaches 23 μs more comparing with the TOF for the receiver in 0°, the time practically double.

The graph also shows the symmetry of the dispersion of the wave for the two halves of sample, between 0°/180° and 180°/0°.

Emitter at -45°

In this case, the emitter is positioned at the side indicated by -45° (equivalent to 135° in Fig.1). This position is marked in relation to the direction of fibers. The time-of-flight from emitter to the transducer in the opposite side is greater when compared to time obtained in the previous case, with value close to 52 μs. The graph of Fig.7(a) shows the averaged values of time to each side. Fig.7(b) shows the position of the transducers.

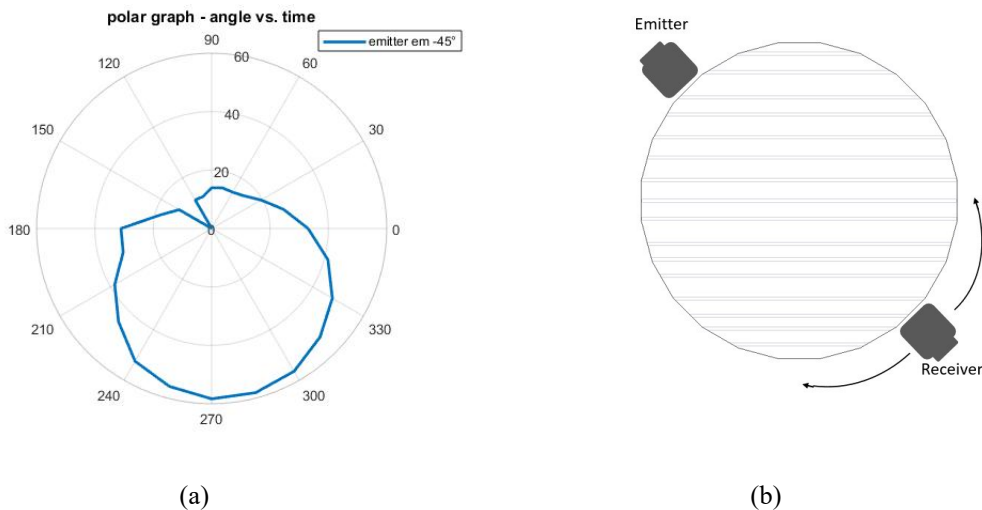


Figure 7 - Results for emitter in -45°. (a) Time vs. position graph (b) Position of the transducer in relation to fiber

As can be seen in the graph of Fig.7(a), the times of flight are greater in this case, and the greatest time occurs in the side indicated as 90° (270°). Moreover, the time-of-flight is the shortest close to sides of the emitting transducer. Particularly, they are short between the sides indicated by 30° and -60° (120°), in the left side of the emitter transducer.

On the other hand, between sides -30° (150°) to 30° (210°) the time also are short, but with difference around of $17 \mu\text{s}$ comparing the angles 30° and 30° (210°) in relation to the emitter. Because of this, symmetry is not expected between the two halves of sample, as occurred in previous case.

It is already known that velocity of wave changes with the variation of angle of fiber. The two tests showed this difference by comparing the times of flight to receiver transducer in opposite and parallel side to the emitter transducer, reinforcing that the wave propagation is more effective in direction of fiber.

Emitter in $+45^\circ$

This analysis considered the emitting transducer positioned at $+45^\circ$ (equivalent to 225° in Fig.1). The graph of Fig.8(a) shows the variation of time-of-flight of longitudinal wave on the different measured sides. Fig.8(b) presents the position of transducers.

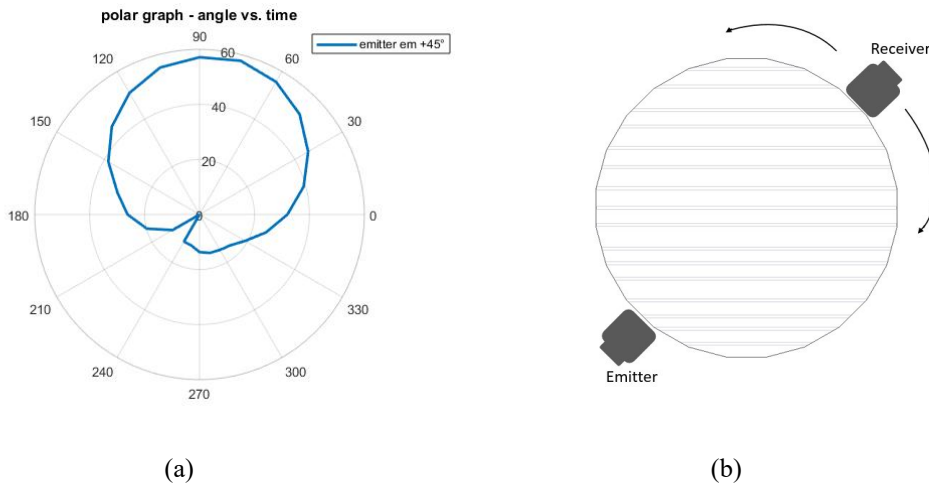


Figure 8 - Results for emitter at $+45^\circ$. (a) Time vs. position graph (b) Position of the transducer in relation to fiber

As noted in graph of Fig.8(a), the lowest times remain on the faces close to emitter transducer, as occurred in the case of the emitter at -45° . The graph also shows the anti-symmetry in relation to the previous graph, in Fig.7(a). For this case, the lowest time occurs to the right side of the face with the emitter transducer, between the angles 60° (240) to -30° (330°). On the left side of the emitter, between faces -30° (150°) to 30° (210°), the times also are short in comparison with those from the side opposite to the emitting transducer. Moreover, there is difference of $19 \mu\text{s}$ comparing the angles -30° (150°) and -30° (330°), of the same aperture with respect to the position of transmitter. This difference confirms that there is not perfect symmetry between the two halves of the sample.

Emitter at 90°

The last direction evaluated was with emitting transducer at 90° (equivalent to 270° in Fig.1). For this case, the fibers are parallel to face of emitter transducer. The graph with times of flight for all sides measured is plotted in Fig. 9(a). And, Fig.9(b) the initial position of transducers.

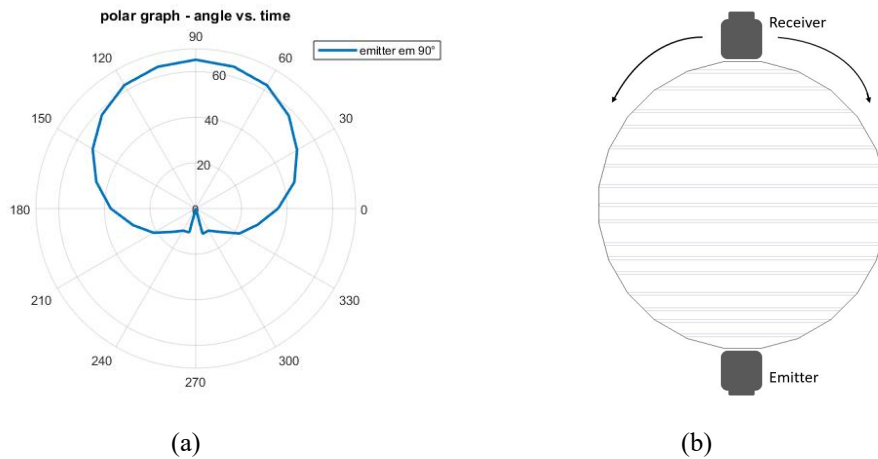


Figure 9 - Results for emitter in 90° . (a) Time vs. position graph (b) Position of the transducer in relation to fiber

In this case the largest time measured is at side 90°, opposite to emitter, reaching more than 60 μs. Compared with other directions measured in the previous cases, this was the slowest velocity obtained for the transducers in opposite faces. Besides, for this case the smaller times are close to faces of the emitting transducer.

The time measured until side 0° was 36 μs and the value obtained to time was 37 μs until side 180°. The standard deviation was about 0,6 μs. In opposition to what was found from the previous results, it looks like there is symmetry of time between the two halves of sample.

It is possible to observe that the experimental results agree with those obtained by Rodvalho (2012), where the highest wave velocity, consequently the shortest time-of-flight, occur when the wave propagates in the direction of the fibers. Consequently, the slowest wave velocity or highest time-of-flight occurs in the direction perpendicular to the fibers. The first and most obvious reason for this can be obtained from the equation proposed by Pao and Gamer (1985), for stress-free orthotropic materials, the larger the C_{11} elastic constant the greater will be the wave velocity. Adapting this concept to composite materials, one can conclude that the higher velocity will occur when the wave propagates in the direction of the fibers.

These results are also related to the speed of phase and group velocity, according to Pearson and Murri (1982). In anisotropic materials, as is the case of composite materials, the wave does not propagate in the normal direction of the wave front, except for the main directions. In other words, the phase and group velocity are only parallel when there is symmetry, in this case at 0 ° and 90 °. This is evidence that the viscoelastic nature of the resin is an important role in wave attenuation and absorption (Biwa et al., 2002).

Signal energy analyses

A second analysis could be done on the energy received by the receiving transducer. As already mentioned for works as Yu et al (2017), in defect detection there are situations where the energy leads to more adequate results than the amplitude of the signal.

The graph for signal $x(t)$ received when transducers were at the opposite side to the transmitter is shown in Fig.10. The energy of the signal is obtained according to Eq. (1), where $x(t)$ is the signal as a function of time.

$$E = \int_{-\infty}^{+\infty} [x(t)]^2 dt \tag{1}$$

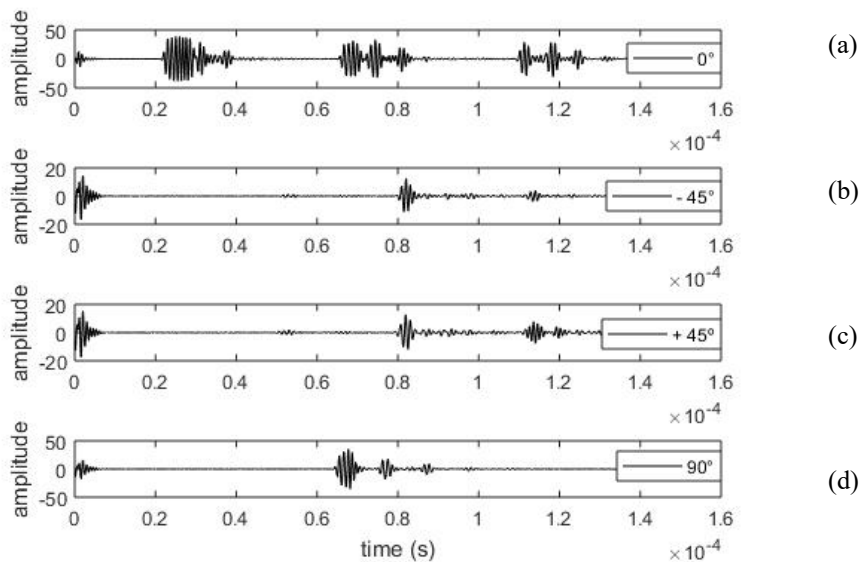


Figure 10 – Graphs with amplitude for receiver transducer parallel to transmitter transducer. (a) Emitter in 0°. (b) Emitter in -45°. (c) Emitter in +45°. (d) Emitter in 90°.

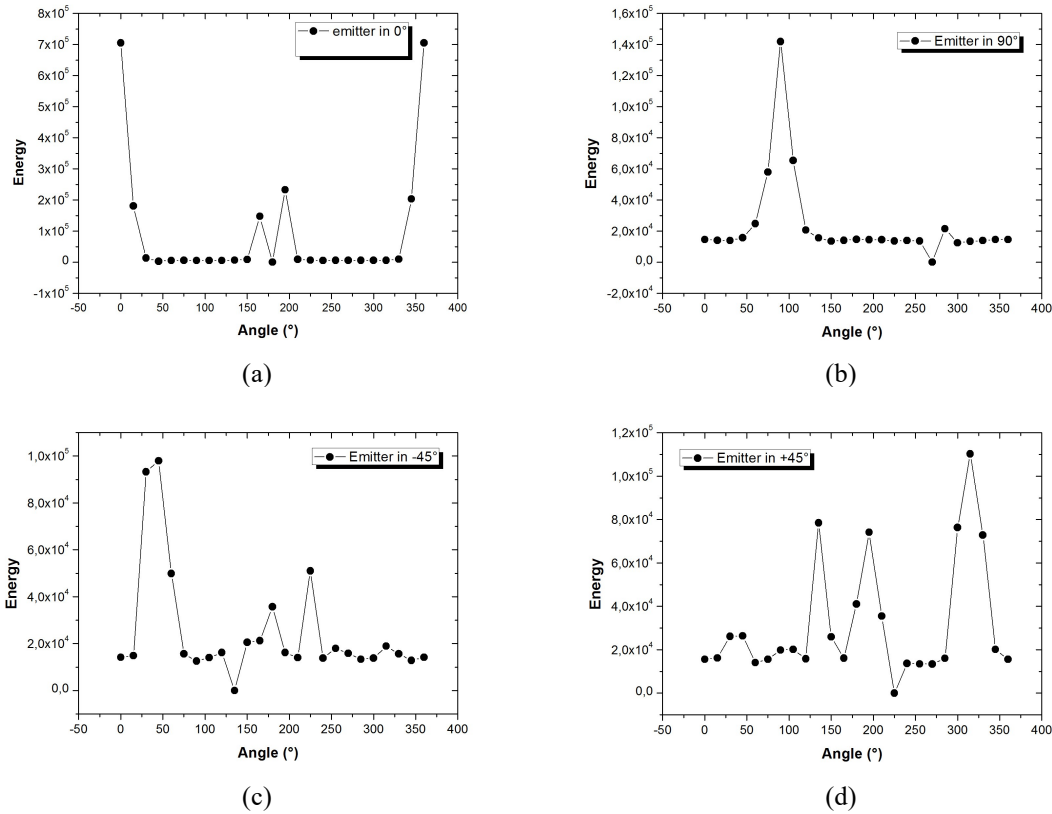


Figure 11 – Presents the graphs of the energy in each place, depending on where the receiver transducer was positioned. (a) Emitter in 0°. (b) Emitter in 90°. (c) Emitter in -45° (d) Emitter in 45°.

To Fig.11(a), the emitter is positioned at 0° (180° according Fig.1) and the highest energy appears at side 0° that is opposite to emitter, followed by adjacent faces, 15° and -15° (345°). The sides near the transmitter transducer, -15° (165°) and 15° (195°) also have a high energy level. The graphs in Fig.11(c) and Fig.11(d) indicate the energy when emitter transducer is in -45° (135°) and +45° (225°), respectively. For these two cases one can see the mirroring of the graphs, noticing that the maximum energy is at sides 45° and 30° following by sides 0° (180°) and 45° (225°) in Fig.11(c). The maximum energy in Fig.11(d) is at side -45° (315°), following by adjacent faces, -60° (300°) and -30° (330°), and at the faces -45° (135°) and 15° (195°). Finally, the Fig.11(b) shows the signal energy when the emitter transducer is at face 90° (270°). The maximum energy is at 90°, following adjacent faces, 75° and -75° (105°), a lower magnitude of energy also appears at -75° (285°), close to emitter.

The results of Fig. 11 are compatible with Biwa et al. (2002), who showed that the viscoelastic nature of the resin exerts great influence on the dispersion, and the fibers effects are negligible. Note that the higher energies occur in regions near the direction of the fiber or perpendicular to it, that is, when the wave is propagating where there is no resin (relative position of the receiver emitter fibers 0°), or when this propagation path has the shortest path through the resin (relative position of the receiving emitter fibers 90°).

According to Biwa et al (2002), when the longitudinal wave travels on a single fiber the wave scattering occurs in the planes ZY, Fig.12, suggesting that the volumetric fraction of fibers has an important effect in the wave scattering. This additional factor explains why the energy of the wave is small when it is transmitted in fiber/matrix interfaces.

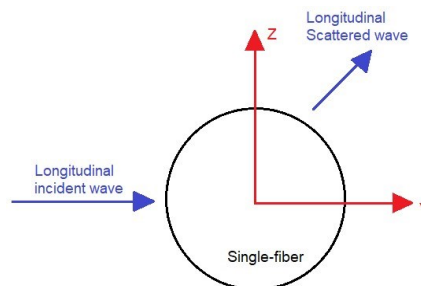


Figure 12 – Single-fiber section and longitudinal wave crossing it.

CONCLUSION

The present work analyzed the dispersion of longitudinal waves in unidirectional composite made of carbon fiber and epoxy resin. The wave source was placed at angles 0° , -45° , $+45^\circ$ and 90° with the fiber direction. This arrangement was possible with a polygonal sample. According to the results, there is symmetry in the propagation of the wave in the sample when the emission of the signal begins at the angle 0° . It also happens when the fibers are perpendicular to the face of emitter, when the signal begins at the angle 90° .

For angles -45° and $+45^\circ$ there is no symmetry and the dispersion wave is anti-symmetry comparing this two cases. This difference shows that the wave tends to travel preferentially in the direction of the fiber. In Santos et al. (2014), the authors stated that temperature variation has very little effect on the velocity of the wave when it is propagating in the direction of the fiber, 0° , and affects significantly the velocity in the direction 45° and 90° , because the wave travels through the resin, which is more sensitive to temperature. The results obtained here confirm this wave trajectory, which is preferred in direction of the fiber, due to the higher resin impedance.

This study shows the dispersion of wave, and this is important to choose better positioning of the transducer, both for inspection of defects and for stress measurement. Stresses causes differences in order of nanoseconds in TOF, and that could be an important factor in the resolution of the ultrasonic method, since the sensitivity is about 3-8 MPa/ns. So, ten nanoseconds could lead to up to 80 MPa, which is normally too much for a measurement method. Because of these arguments, the correct alignment of the probes during stress measuring in composites is fundamental to reach liable results.

REFERENCES

- Baudouin, S.; Hosten, B. Immersion ultrasonic method to measure elastic constants and anisotropic attenuation in polymer-matrix and fiber-reinforced composite materials. *Ultrasonics*, v. 34, n. 2-5, p. 379–382, 1996.
- Biwa, S; Idekoba, S. Ohno, N. wave attenuation in particulate polymer composites: independent scattering/absorption analyses and comparison to measurements. *Mechanics of Materials*, 34, 671-682, 2002
- Hughes DS, Kelly JL. Second-Order Elastic Deformations of Solids. *Phys Rev* 1953; 92: 1145–1150.
- Pao YH, Gamer U. Acoustoelastic waves in orthotropic media. *J Acoust Soc Am* 1985; 77: 806–812.
- Pearson, L.H. and Murri, W.J. Measurement of ultrasonic wavespeeds in off-axis directions of composite materials. *Review of progress in quantitative nondestructive evaluation*, v. 1, p. 1056-1064, 1982.
- Rodvalho, T.G. Medição da Velocidade da Onda Ultrassônica Longitudinal em Compósitos de Fibra de Carbono/Epóxi. 2012. Dissertação (Mestrado) – Faculdade de Engenharia Mecânica, Universidade Estadual de
- Santos AA, Ambiel LB, Garcia RH, et al. Stress analysis in carbon/epoxy composites using Lcr waves. *J Compos Mater* 2014; 48: 3425–3434. Campinas, Campinas.
- Santos AA, Bray DE. Comparison of Acoustoelastic Methods to Evaluate Stresses in Steel Plates and Bars. *J Press Vessel Technol* 2002; 124: 354.
- Thurston RN, Brugger K. Third-order elastic constants and the velocity of small amplitude elastic waves in homogeneously stressed media. *Phys Rev* 1964; 133: 1604–1610.
- Toupin RA, Bernstein B. Sound Waves in Deformed Perfectly Elastic Materials. Acoustoelastic Effect. *J Acoust Soc Am* 1961; 33: 216–225.
- Yu, X; Ratassepp, M; Fan, Z. Damage Detection In Quasi-Isotropic Composite Bends Using Ultrasonic Feature Guided Waves. *Composites Science And Technology*. 120-129, 2017

RESPONSIBILITY NOTICE

The authors are the only responsible for the printed material included in this paper.